PERGAMON

Applied Radiation and Isotopes 50 (1999) 375–380

Applied Radiation and Isotopes

Characteristics of the solid state nuclear detector CR-39 for neutron radiography purposes

Reynaldo Pugliesi *, Marco A. Stanojev Pereira, Marco A.P.V. de Moraes, Mário O. de Menezes

Divisão de Física Nuclear, TFF, Instituto de Pesquisas Energéticas e Nucleares, IPEN/CNEN-SP, Caixa Postal 11.049, Pinheiros, CEP 05422-970 Sao Paulo, SP, Brazil

Received 2 December 1997; received in revised form 13 April 1998; accepted 14 April 1998

Abstract

The solid state nuclear track detector CR-39, together with a natural boron converter screen have been used as an image-detector system for neutron radiography purposes. In order to determine its radiographic characteristics, the image-detector system was irradiated up to neutron exposures around 6×10^{10} n/cm^2 in a radiography facility installed at the IEA-R1 Nuclear Research Reactor. The detectors were chemically etched in a KOH (30%) aqueous solution at 70°C. The best radiography conditions were obtained for neutron exposures ranging from 1×10^9 to 2×10^{10} n/cm^2 and for 25 min etching time. The present results were compared with those determined for other track detectors and discussed according to the theory of the image formation in solid state nuclear track detectors. This theory is based on the optical properties of a single track.

1. Introduction

The ability of solid state nuclear track detectors (SSNTD) to register local damages of individual radiation events and their insensitivity to visible light, β and γ radiations are some of the characteristics that makes these detectors attractive for neutron radiography (NR) purposes (Fleischer et al., 1975; Lferde et al., 1984).

In the NR technique, the sample is irradiated in an uniform neutron beam and a screen converts the transmitted thermal neutrons to ionizing radiation which is able to induce damages into the SSNTD. Damages can also be induced by direct collision between fast neutrons and the bonded hydrogen of the detector. This contribution should be evaluated for the characterization of SSNTD for NR studies. By means of an adequate chemical etching the damages are enhanced, giving rise to tracks which will form a visible image (Lferde et al., 1984). Ilic has proposed a theory, based on the optical properties of a single track, which explains the image formation process in SSNTD (Ilic and Najzer, 1990a,b,c,d).

The objectives of the present work were to investigate the main characteristics of the SSNTD CR-39 with a natural boron converter screen, for neutron radiography purposes. The optimum etching times and neutron exposures for the best image contrast and resolution have been determined. The present results are compared with those previously determined for CN-85 (Assunção et al., 1992) and Makrofol-E (Assunção et al., 1994), employing the same methodology used in this work and are discussed according to Ilic's theory.

2. Experimental

The NR facility is installed at the radial beam-hole #08 of the 2MW pool type IEA-R1 Nuclear Research Reactor (de Menezes, 1994). The main characteristics of the neutron beam are listed in Table 1. The ex-

* Corresponding author. E-mail: pugliesi@curiango.ipen.br.

0969-8043/99/$ - see front matter
PII: S0969-8043(98)00092-X

Table 1
Main characteristics of the neutron beam

Neutron flux at the sample	3×10^6 n/s·cm^2
Collimation ratio (L/D)	70
n/γ ratio	$>10^5$ n/cm^2·mR
Beam diameter	20 cm
Au–Cd ratio	>150

posures were performed by using an aluminum cassette containing the SSNTD and the converter screen in a tight contact during irradiation. This set was attached to a sample holder and was led to the irradiation position by a remote control system.

The SSNTD CR-39 is a polycarbonate, 600 μm thick, manufactured by Pershore Mouldings (England). The converter screen, manufactured by Kodak Pathè (French), is a plastic backing single coated with a natural boron layer 65 μm thick. The damages in the detector are induced by the products of the nuclear reaction ^{10}B(n, α)^{7}Li (α-energy = 1.47 MeV; Li-energy = 0.84 MeV) for which the intrinsic registration efficiency is near unity (Ilic and Najzer, 1990c).

The chemical etching was performed in a KOH (30%) aqueous solution at a constant temperature of 70°C. The etched CR-39 detectors have been analysed in a TV monitor-camera system coupled to an optical microscope as well as in a Jarrel-Ash optical microphotometer. The former was employed for track inspection and the latter for light transmission readings.

3. Data analysis

3.1. Track size

The optical density distribution across a single track, varies with the track shape (Antanasijevic et al., 1977; Ilic et al., 1986; Ilic and Najzer, 1990a,d). In this way, track size plays an important role in the resolution and contrast of the radiographic image. Fig. 1 shows the track diameters obtained for the CR-39 detector as a function of the etching time varying in the interval $10 < t_e < 65$ min. The measurements were performed in the TV monitor-camera system, employing the optical microscope with 1500 × -magnification. The track diameter readings were obtained directly onto the monitor screen, using a previously calibrated length scale. Each point in the graph represents an average of diameters for 10 distinct tracks and the obtained values ranged from $(1.0 \pm 0.1) < \phi_t < (4.1 \pm 0.2)$ μm. The minimal track diameter value was limited only by its sharp visualization onto the screen. These measurements were carried out at a negligible track overlapping condition which was achieved for neutron exposure around $E \sim 9 \times 10^7$ n/cm^2.

3.2. Track production rate

This parameter is defined as the track to neutron conversion efficiency of the image-detector system. The conversion efficiency was determined from the slope of the straight line fitted to the experimental data points of track density as a function of the neutron exposure. The track densities have been obtained by counting, onto the monitor screen of the TV-camera system, the tracks at fixed areas of the CR-39 detector and subtracting from these values the background track density. Such counting were performed in the maximal conversion efficiency condition which was achieved for etching times greater than 20 min, as can be seen in Fig. 2. The selected etching time was $t_e = 25$ min where the background track density obtained was about 2×10^5 tr/cm^2. The results are shown in Fig. 3 and the obtained track production rate was tr/n = $(7.9 \pm 0.3) \times 10^{-3}$.

3.3. Optical density

The optical density, D_{op}, is defined as:

$$D_{op} = \log \frac{I_0}{I}$$

where I_0 and I are the intensities of the incident and transmitted light through the detector, respectively. Fig. 4 shows the trend of the characteristic curves for

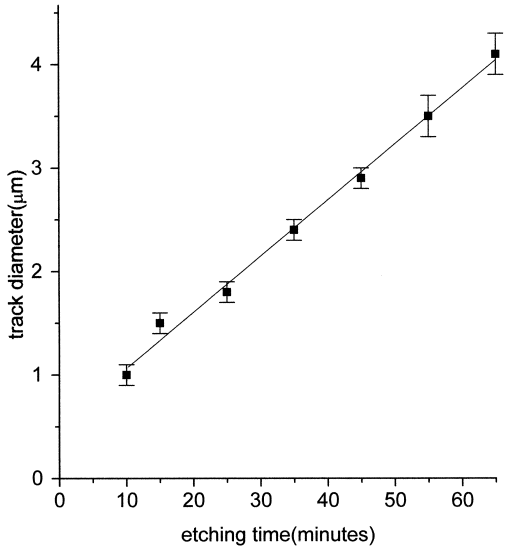

Fig. 1. Growth of the track diameter as a function of the etching time.

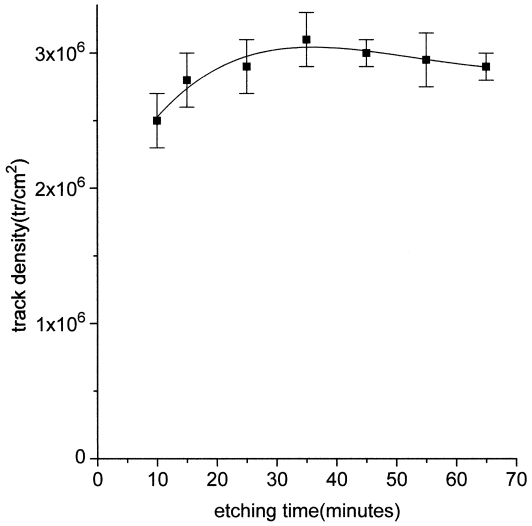

Fig. 2. Variation of the track density as a function of the etching time.

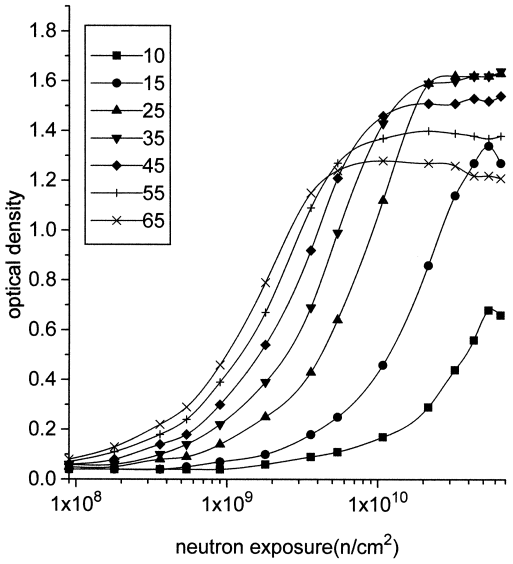

Fig. 4. Characteristic curves for CR-39, for thermal neutrons.

the optical density readings as a function of the neutron exposures and etching times varying from $1 \times 10^8 < E < 6 \times 10^{10}$ n/cm^2 and $10 < t_e < 65$ min, respectively. These readings were carried out in the microphotometer using a scanning beam width of 3 μm. According to the theory proposed by Ilic, the behavior of the curve for $t_e = 25$ min, for example, can be explained as follows: for neutron exposure up to $E \cong 6 \times 10^8$ n/cm^2, the track density is relatively low to produce appreciable optical density above the detector background ($D_{op} \sim 0.04$); for 1×10^9 n/cm$^2 < E < 2 \times 10^{10}$ n/cm^2 a competition between single track production (responsible by optical density increasing) and track overlapping (responsible by optical density decreasing) leads to an increasing of the optical density; for $E > 2 \times 10^{10}$ n/cm^2 track overlapping becomes predominant and the optical density shows an approximately constant trend for a small interval and will decrease for higher neutron exposures (Ilic and Najzer, 1990a).

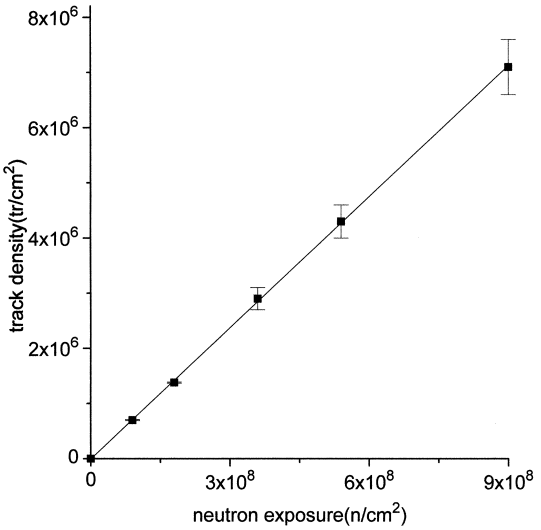

Fig. 3. Growth of the track density with neutron exposure for etching time $t_e = 25$ min.

The image contrast, defined by $G = dD_{op}/d(\log E)$, was determined by fitting straight lines to the steeper region of the characteristic curves and the results have shown that increasing the etching time the contrast increases, reaching the maximal value of 1.51 ± 0.01 for $t_e = 25$ min where the track production rate is maximum (Fig. 2). The contrast decreases for $t_e > 25$ min as a consequence of the track overlapping, which leads to a slower increasing of the optical density (Ilic and Najzer, 1990a).

The fast neutron contribution to the image formation was also verified by irradiating the detectors without the converter screen. In Fig. 5 some characteristic curves, obtained following the same procedures employed with converter screen and for three etching times, are shown. As can be seen the optical density presents some contribution only for $t_e = 65$ min and $E > 2 \times 10^{10}$ n/cm^2.

3.4. Resolution

In radiography studies, the resolution is usually defined as the distance that must separate two objects before they can be distinguished from each other (Ilic and Najzer, 1990d). In the theory of the image formation in SSNTD, the resolution is quoted in terms of the intrinsic unsharpness of the image-detector system.

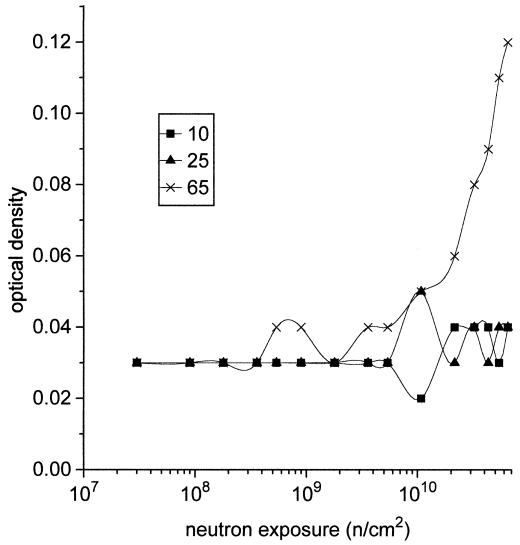

Fig. 5. Characteristic curves for CR-39, for fast neutrons.

This parameter has been determined by scanning the image of a gadolinium knife-edge test object 0.127 mm thick, irradiated in a tight contact with the image-detector system. Such scanning was performed by using the microphotometer and the edge spread function ESF = $A + B{\cdot}\arctan(C^{1/2}{\cdot}(X-D))$ has been fitted to the resulting optical density distribution data. In this equation A, B, C and D are free parameters and X is the scanning coordinate (Wade et al., 1987; Wrobel and Greim, 1988). A typical fit is shown in Fig. 6. The term $U_T = 2{\cdot}C^{-1/2}$ is the total unsharpness for the NR facility and corresponds to the FVHM (full width at half maximum) of the differentiated ESF (a Lorentz distribution). The total unsharpness results from the combined effect of intrinsic unsharpness (U_I) due to the image-detector system and geometrical unsharpness (U_G) due to the neutron beam angular divergence contributions. They are related by the equation $(U_T)^n = (U_I)^n + (U_G)^n$ (Hawkesworth, 1977). For the present irradiation geometry the distance of the test object to the converter screen was about 730 μm and the geometrical unsharpness was $U_G \cong 10$ μm. The intrinsic unsharpness values were calculated by using the above equation with $n = 1.5$, since theoretically, the unsharpness ratio $U_G/U_I \sim 1$ (Harms and Zellinger, 1977). The obtained results, for the neutron exposure interval $9 \times 10^8 < E < 2 \times 10^{10}$ n/cm^2 and for the etching times 15, 25, 45 and 65 min are shown in Fig. 7.

The theory of the image formation in SSNTD states that U_I is independent of E and remains constant at a minimum value $U_I \sim 0.8 \times R$ (R is the range of the reaction products in the converter screen), for a negligible track overlapping condition and for diameters $\phi_t < R$ (Ilic and Najzer, 1990d). The greater the neutron exposure, the greater track overlapping and in this case U_I increases linearly with the logarithm of exposure. As can be seen in Fig. 7 the obtained values for U_I have shown a similar trend. A mean value of (13 ± 3) μm was obtained for the intrinsic unsharpness, for track diameters $\phi_t < R$, i.e. 1.3, 1.8, 3.4 and 4.5 μm, and in low track overlapping condition, i.e. for 15 and 25 min etching times in the neutron exposure interval $1 \times 10^9 < E < 2 \times 10^{10}$ n/cm^2 as well as for 45 and 65 min in $E = 9 \times 10^8$ n/cm^2, respectively. Since for the present converter screen $R \sim 9$ μm, theoretically the

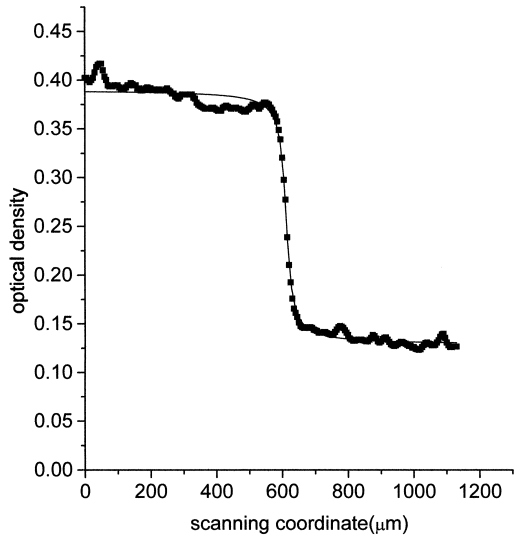

Fig. 6. Optical density distribution for a gadolinium knife edge test object and the fitted edge spread function. Data obtained for etching time, $t_e = 25$ min.

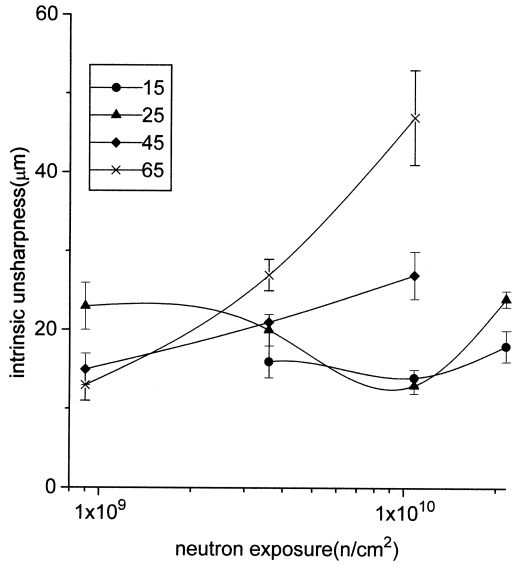

Fig. 7. Intrinsic unsharpness behavior as a function of the neutron exposure for four etching times.

Table 2
Comparison of the main radiographic characteristics for the CN-85, Makrofol-E and CR-39 detectors

SSNTD	Etching time (min)	Track diameter (μm)	(tr/n) $\times 10^{-3}$	Contrast G	Unsharp· U_I (μm)
CN-85	7	1.4	(7.8 ± 0.3)	(1.82 ± 0.06)	15
Makrofol-E	5	1.4	(5.8 ± 0.4)	(0.73 ± 0.07)	15
CR-39	25	1.8	(7.9 ± 0.3)	(1.51 ± 0.01)	13

best value for U_I is approximately 7 μm. This discrepancy can be attributed to the contact irregularities at the CR-39/converter screen interface as well as to the neutron beam and converter screen inhomogeneities. The former leads to an α-particle scattering into the irregular remaining air layer at the interface and the latter to the presence of small track clusters which have been observed by microscope analysis even at the low track overlapping condition (Assunção et al., 1992).

4. Conclusions

According to the results obtained in this work, the best radiographic conditions for the SSNTD CR-39, in terms of contrast and resolution, were achieved for an etching time of $t_e = 25$ min in a KOH (30%) solution at 70°C and for a neutron exposure interval $1 \times 10^9 < E < 2 \times 10^{10}$ n/cm^2. For such conditions the following characteristics were achieved: track diameter (1.8 ± 0.1) μm; track to neutron conversion efficiency $(7.9 \pm 0.3) \times 10^{-3}$; image contrast (1.51 ± 0.01); mean resolution 13 μm; insensitivity for neutron exposures up to $\sim 6 \times 10^8$ n/cm^2. Furthermore the fast neutron contribution in the image formation is negligible since its optical density becomes significant for etching times around 65 min and for exposures above 2×10^{10} n/s·cm^2, i.e. out of the limits obtained for the best radiography conditions.

It was verified that the image contrast increases with the etching time up to $t_e = 25$ min and decreases for $t_e > 25$ min. This behavior has been explained in terms of the track production rate and optical density distribution across overlapped tracks, respectively.

It was also verified that the behavior of the intrinsic unsharpness is qualitatively in good agreement with the one foreseen by the theory of the image formation in SSNTD. However, the average of its lower values is almost twice higher than the theoretical one and, as mentioned above, this can be a consequence of α-particle scattering as well as the presence of small track clusters. In this case the employment of an air evacuated cassette, and improvements concerning the neutron beam and converter screen homogeneities will provide unsharpness values closer to the theoretical one.

Table 2 shows the main radiography characteristics for the SSNTD, CR-39, CN-85 and Makrofol-E, which have been determined by employing the same methodology. CR-39 presents a contrast somewhat lower than CN-85 because the mean track diameter of the former is somewhat greater. However CR-39 shows a contrast about twice higher than that for Makrofol-E This is a consequence of its higher track production rate and higher transparency to visible light since their chemical bondings are weaker and Makrofol-E is a translucent material (Matsumoto et al., 1986; Assunção et al., 1994). For the three SSNTD, the obtained intrinsic unsharpness values as well as their discrepances with the theoretical one are very similar. This can be explained by taking into account that for these image-detector systems, track overlapping occurrences as well as α-particle scattering are nearly the same for the experimental conditions in which the unsharpness have been evaluated.

References

Antanasijevic, R., Todorovic, Z., Stamatovic, A., Miocinovic, D., 1977. Factors affecting the sensitivity of plastic detectors to ionizing α-particle registration. Nucl. Instrum. Methods 147, 139–140.

Assunção, M.P.M., Pugliesi, R., de Menezes, M.O., 1992. Characteristics of the solid state nuclear track detector CN-85 for neutron radiography. Proceedings of the Fourth World Conference on Neutron Radiography. San Francisco, California, USA, May 10–16.

Assunção, M.P.M., Pugliesi, R., de Menezes, M.O., 1994. Study of the neutron radiography characteristics for the solid state nuclear track detector Makrofol-E. Appl. Radiat. Inst. 45 (8), 851–855.

Fleischer, R. L., Price, P.B., Walker, R.M., 1975. Nuclear Tracks in Solids-Principle and Applications. University of California, Berkeley, California, USA.

Harms, A.A., Zellinger, A., 1977. A new formulation of total unsharpness in radiography. Phys. Med. Biol. 22 (1), 70–80.

Hawkesworth, M.R., 1977. Neutron radiography: equipments and methods. Atom. Energy Rev. 152, 169–220.

Ilic, R., Rant, J., Humar, M., Somogyi, G., Hunyadi, I., 1986. Neutron radiographic characteristics of M4-ND type (allyl-diglycol-carbonate) nuclear track detectors. Nucl. Tracks 12 (1–6), 933–936.

Ilic, R., Najzer, M., 1990a. Image formation in track-etch detector. I. The large area signal transfer function. Nucl. Track Radiat. Meas. 17, 453–460.

Ilic, R., Najzer, M., 1990b. Image formation in track-etch detector. II. The space-dependent transfer function in thin detectors. Nucl. Track Radiat. Meas. 17, 461–468.

Ilic, R., Najzer, M., 1990c. Image formation in track-etch detector. III. The space-dependent transfer function in thick detectors. Nucl. Track Radiat. Meas. 17, 469–473.

llic, R., Najzer, M., 1990d. Image formation in track-etch detector. IV. Image quality. Nucl. Track Radiat. Meas. 17, 475–481.

Lferde, M., Lferde, Z., Monnin, M. et al, 1984. Neutron radiography with track detectors. Nucl. Track Radiat. Meas. 8 (14), 497–499.

Matsumoto, G., Murata, N., Suzuki, S., Matsumoto, M., Ohkubo, K., Ikeda, Y., 1986. Track-etch neutron radiography with a new boron carbide converter. Nucl. Technol. 72, 201–211.

de Menezes, M.O., 1994. Development and application of the neutron radiography technique by direct and indirect conversion methods. M.Sc. Thesis. Nuclear Energy National Commission. IPEN-CNEN/SP BRAZIL.

Wade, J., Larson, R., Larson, H.A., 1987. Radiography experiments at Argonne National Laboratory. Nucl. Technol. 76, 408–419.

Wrobel, M. and Greim, L., 1988. Resolution Functions and Unsharpness in Neutron Radiography. Geesthacht, German, GKSS (GKSS 88/e/12).